An Autonomous Low Earth Orbit Smallsat Mission and Payload Design for Microdebris Deorbiting via Laser Ablation

Melik C. Demirel,[*] Joseph W. Healy,[†] Kiara N. Cornell,[‡] George S. Harmon,[§] Denver Nazareth,[**] and Claire L. Shaw[††]

The Pennsylvania State University, University Park, Pennsylvania, 16802, USA

The Watchdog mission and payload comes in response to the increasing need to innovate and advance In-space Servicing, Assembly, and Manufacturing potential and ability. As humanity expands its presence in space, the demand for methods to improve space mission sustainability has consequently increased. One impending factor that is projected to limit future space exploration and satellite operations is the growing amounts of space debris orbiting the Earth. There are tens of millions of microdebris in orbit around the Earth, varying from one centimeter to a few millimeters in size, which can cause catastrophic damage spacecraft in low earth orbit. The overarching goal of the Watchdog payload is to move microdebris particles into sub-orbital trajectories using optical power transmission in the form of a laser. The momentum change caused by laser ablation on targeted debris particles can be used to slow them to suborbital trajectories, where they may disintegrate in the atmosphere. This report outlines the mission of combining a high-power laser and tracking technology to detect and redirect debris on close approach with the satellite. In addition, this report details the thermal and power considerations, as well as a physical simulation of debris redirection.

I. Nomenclature

E	=	laser pulse energy
E	=	Young's modulus
F	=	force
f	=	laser pulse repetition frequency
FS	=	factor of safety
I	=	moment of inertia
L	=	length
ℓ	=	size (in a dimension)
M_E	=	Earth's mass
m	=	mass
P_a	=	average power ($E \cdot f$, if a pulse laser)
P_p	=	E/τ peak power
Δv	=	change in velocity
λ	=	laser wavelength
τ	=	laser pulse duration

II.Introduction

As humanity expands its presence in space, the demand for sustainable mission practices grows increasingly urgent. In-space Servicing, Assembly, and Manufacturing (ISAM) has emerged to support long-term space sustainability through autonomous, on-orbit capabilities. One of the most significant threats to future satellite operations that ISAM technologies aim to address is the rapid accumulation of space debris in Earth's orbit. Tens of millions of microdebris

[*] Undergraduate student, Department of Aerospace Engineering, melikcdemirel@gmail.com, AIAA member.
[†] Undergraduate student, Department of Aerospace Engineering, josephhealy28@gmail.com, not an AIAA member.
[‡] Undergraduate student, Department of Aerospace Engineering, not an AIAA member.
[§] Undergraduate student, Department of Aerospace Engineering, not an AIAA member.
[**] Undergraduate student, Department of Aerospace Engineering, not an AIAA member.
[††] Undergraduate student, Department of Aerospace Engineering, not an AIAA member.

particles, ranging from a few millimeters to about one centimeter in size, now orbit the planet. Despite their small size, these particles can impart substantial kinetic energy, with impacts equivalent to a pitched baseball or even a falling anvil. A three-millimeter fragment alone can deliver force comparable to a flying bullet. Such collisions have the potential to critically damage satellite infrastructure or even cause total mission failure.

Studies show that microdebris can reduce satellite lifespans by 3–13% [1]. These effects are detailed in Table 1. This reduction in operational life translates directly into increased costs. Replenishment expenses are projected to rise by 2–15%, with large constellations facing the greatest financial burden due to frequent and costly replacements. These projected cost increases are also described in Table 1. Microdebris pollution could cost the space industry billions of dollars [1]. Without mitigation, such compounding financial pressures could jeopardize the economic viability of future ISAM programs and risk the long-term sustainability of satellite infrastructure.

Table 1 Decrease in satellite lifespans and increase in costs because of microdebris impacts [1].

		Satellite / Constellation Type		
		Small (Government)	*Medium (Commercial)*	*Large (Commercial)*
No Debris	*Mean Lifetime (years)*	5.7	9	12
	Replenishment Cost ($Billion)	20.1	16.9	7.9
Fatal Impacts Only	*Mean Lifetime (years) &* *Percent Reduction (2010-2040)*	5.5 – 5.6 2.3 – 2.1%	8.5 – 8.6 5.0 – 4.6%	11.5 – 11.6 5.7 – 5.1%
	Replenishment Cost ($Billion)	20.4 (2% increase)	17.7 (5% increase)	8.6 (8% increase)
All Impacts	*Mean Lifetime (years) &* *Percent Reduction (2010-2040)*	5.4 – 5.5 4.4 – 3.4%	8.2 – 8.3 8.9 – 7.6%	10.6 – 11.2 13.1 – 8.3%
	Replenishment Cost ($Billion)	20.8 (4% increase)	18.4 (9% increase)	9.1 (15% increase)

This paper overviews the proposed *Watchdog* mission, including the payload concept, subsystem designs, and supporting analyses that advance a novel approach to orbital debris mitigation. The mission centers around the design of a payload hosted aboard the Blue Canyon Technologies (BCT) X-Sat Venus-Class Bus (VCB). The *Watchdog* payload is intended to demonstrate a chain of autonomous, on-orbit operations aligned with ISAM principles, with the objective of enabling sustainable defense against microdebris threats. The Watchdog payload is designed to achieve this by imparting a momentum change to individual debris particles using optical power transmission, particularly laser ablation. The objective is not to destroy debris, which could generate even smaller, more hazardous fragments, but to ablate its surface just enough to push it into a suborbital trajectory, where it will re-enter Earth's atmosphere and disintegrate safely. Furthermore, the payload must acquire, track, and continuously monitor target debris, while precisely delivering energy through ablation (and radiation pressure). The system requires coordinated reorientation of the optical transmission unit, sensors, and spacecraft bus to maintain accurate engagement with the target.

The payload and bus have been modeled using computer-aided design (CAD) software. A comprehensive analysis of launch constraints led to the selection of the Minotaur IV launch vehicle, operating out of Cape Canaveral. Preliminary power and mass budgets have been developed, with updates continuing as subsystem integration evolves. Orbital analysis performed in Ansys Systems Tool Kit (STK) has supported logistics planning and maneuvering strategy, while a custom MATLAB simulation enables long-term trajectory modeling of redirected debris. On the communications front, C&DH has completed an uplink and downlink budget with positive link margins, as well as a flow diagram showing the path of data.

Several key areas remain in active development. A laser trade study evaluates suitable commercial systems for optical energy delivery. A list containing over three hundred commercially available lasers has been compiled to assist in part selection. However, the optimal laser parameters for the mission have yet to be determined, but methodology for doing is provided. Power and thermal subsystems continue to refine internal energy distribution and heat management strategies. Coordination between orbital mechanics and the spacecraft's attitude control system is still in progress, aimed at developing a robust GNC model. Meanwhile, C&DH must finalize data transmission strategies and determine the onboard computing specifications necessary to support autonomous operations.

This whitepaper details the Watchdog mission concept, current progress, subsystem designs, and future work. By demonstrating an ISAM-based solution to the microdebris challenge, the *Watchdog* mission contributes a critical step toward the safe and sustainable future of spaceflight.

A. Needs

Microdebris in space poses a threat to other missions. Fig. 1 shows that as the number of objects launched into space grows, as does the amount of space debris orbiting the Earth.

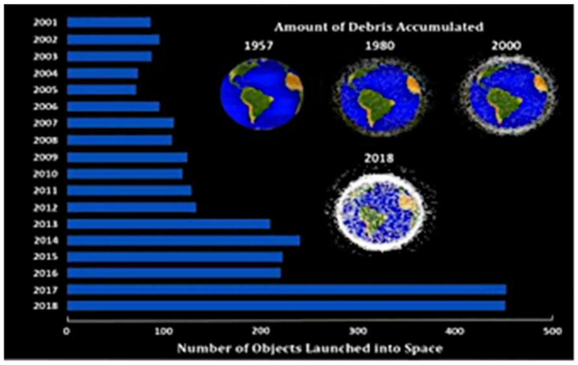

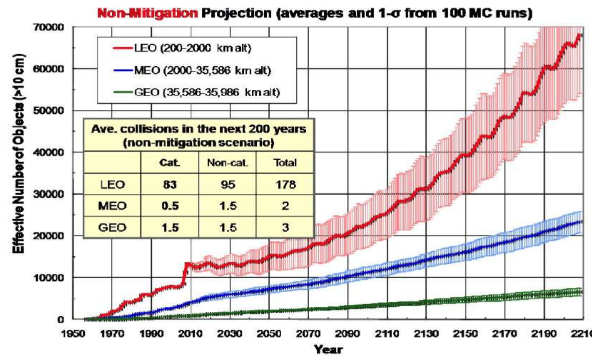

Fig. 1 Debris Accumulation (Left) and Future Projection (Right) [1].

With debris projected to grow, there needs to be a solution to reduce the quantity of debris. A single impact from even the smallest debris particles has catastrophic levels of energy, as described in Table 2.

Table 2 Impact consequences of varying microdebris sizes. [2].

Debris Size	Mass (g) aluminum sphere	Kinetic Energy (J)	Equiv. TNT (kg)	Similar in Energy to	Quantity	Currently Trackable?
1 mm	0.0014	71	0.0003	Pitched baseball	Tens of millions	No
3 mm	0.038	1910	0.008	Bullets	Millions	No
1 cm	1.41	70700	0.3	Falling anvil	Hundreds of thousands	No
5 cm	176.7	8840000	37	Hit by bus	Tens of thousands	Mostly not
10 cm	1413.7	70700000	300	Large bomb	Tens of thousands	Mostly yes
> 10 cm	1400 – 500,000,000	< 10^13	< 3,000,000	Very large bomb	Thousands	Cataloged

Currently, a long-range and high coverage solution does not exist for reducing small debris particles. To improve spacecraft sustainability, cost, and mission life, there needs to be a solution for the rising microdebris problem. The Watchdog mission has investigated the use of long-range lasers to push microdebris into suborbital trajectories via ablation.

B. Goals, Objectives, and Mission Statement

Optical power transmission shall be used to satisfy the ISAM initiative for defense against microdebris particles in space. The system contains three operations (or objectives) executed in parallel:

- *Acquire, track, and actively monitor a target to validate power delivery.*
- *Continuously reorient the optical transmission device, detectors, and the bus satellite.*
- *Deliver optical power, moving debris via laser ablation or radiation pressure.*

Together, these formulate the *Watchdog* mission.

C. Macro-Level Mission Architecture

To organize the concepts, a graphic, as shown in Figure 2 was created to show an overview of operations. It details the steps involved between the initial deployment and power delivery phase.

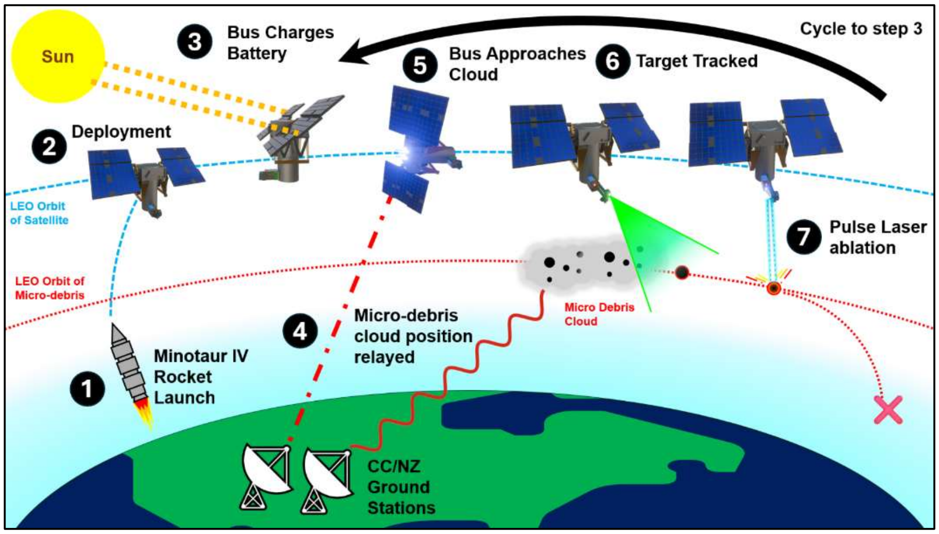

Figure 2 Mission architecture: overview of operations.

The general phases of operations are (1) the spacecraft's launch into target orbit, (2) the deployment of the payload, (3) the battery charging phase, (4) micro debris cloud detection from the Space Fence ground station, (5) rendezvous with the target debris cloud, (6) acquiring a debris target, and (7) debris target redirection using the laser. Phases (3)-(7) are repeated throughout the mission. Once the spacecraft has reached its end of life, it will deorbit using the bus propulsion. Throughout each phase, the BCT X-sat Venus Class bus will relay information to the payload device from the ground station when necessary. Additionally, the payload will operate on autonomous subroutines chosen by the ground station without much manual input thereafter.

III. Mission Overview

D. Payload Description and Operations

The payload consists of several components: the Optics Device, the Target Monitor, Command and Data Handling (C&DH), Thermal, Structures, and Guidance Navigation and Control (GNC), which are allocated to unique team members as subsystem leads. The Venus class bus includes separate Communications, Power, C&DH, Thermal, Structures, Propulsion, and GNC subsystems. Other subsystems or categories are the Ground System, Launch Vehicle (LV), Astrodynamics, Computer-Aided Design (CAD), and systems integration. Details of the masses and power requirements of the main systems on the payload are included in Table 3.

Table 3 Payload mass and power budget.

Component	Mass (kg)	Nominal Power (W)	Peak Power (W)
Laser	2.0	66.0	625.0
Tracking Sensors	30.0	150.0	155.0
Power	1.0	-	-
Thermal	10.0	50.0	150.0
Structures	10.0	-	-
GNC+C&DH	1.5	5.0	15.0
20% Margin	54.5	54.2	189.0
Payload Total	65.4	325.2	1134

The micro-level mission architecture, as shown in Fig. 3, shows the deployment and use of the payload during the mission. The key features of the payload include the laser, galvanometer, Light Detection and Ranging (LIDAR) detector, and Infrared (IR) camera.

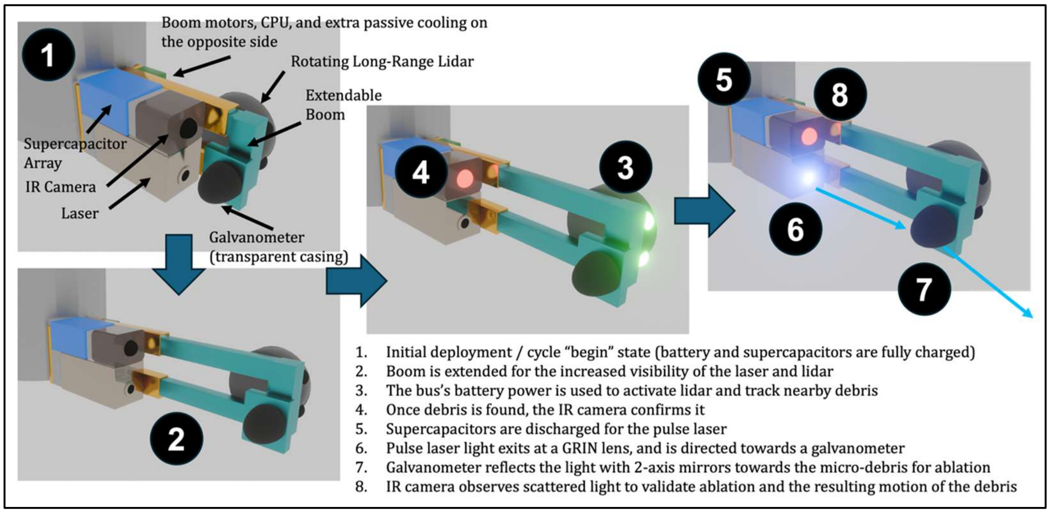

Fig. 3 Micro-level mission architecture (payload only).

These features of the payload will detect debris and direct the laser to the target. Additionally, the payload will include supercapacitors, computers, and passive cooling systems to support the payload's operation. The micro-level architecture shows the general deployment of the payload, where a boom containing the LIDAR tracker and galvanometer are extended away from the payload for a better field of view. Once fully deployed, the LIDAR sensor will sweep over an area by spinning the optic. It will scan for particles in front of the payload. Once an object is found, it will use the IR camera to verify the particle size and type. Simultaneously, onboard processing will determine the relative position and velocity of the particle so the laser can be accurately directed to its position. The galvanometer will perform the laser redirection, and the laser system will be activated during the encounter. Once the debris is out of range, or the laser cannot apply an ablative force opposite the particle's velocity vector, the laser will stop, and the LIDAR will proceed to find new targets. If power is insufficient for the ablation, the spacecraft will wait for direct sunlight and wait until the batteries and capacitors are charged.

E. Payload CAD

The following section lists the necessary components needed in the payload to complete the prescribed mission. Table 4 lists the fundamental components for debris detection, tracking and ablation, and thermal and power and power management.

Table 4 Payload bill of materials.

Item No.	Part Name	Description	Quantity
1	Payload Box	Aluminum 1060 container payload	1
2	Boom Motor	Rotational motor for boom	1
3	Boom	Translatable extension	1
4	Cylindrical Lidar	Debris tracker	1
5	IR Camera	Camera for debris detection	1
6	Superconductors Array w/ Thermal Shields	Power transmitter	1
7	Shock Absorbers	Force dampeners	2
8	CPU	Payload computer	1
9	Galvanometer	Laser positioner	1
10	Laser	Debris ablation tool	1

Fig. 4 shows the arrangement of these components within the required 16.4-inch x 17-inch x 27-inch payload box, as well as the full rendering of the payload attached to the host spacecraft.

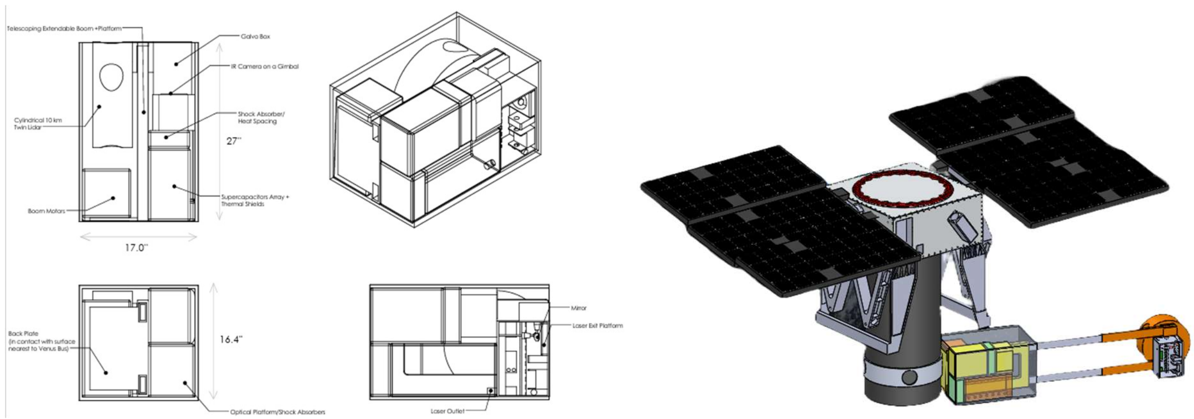

Fig. 4 Payload 3 view (left) and full CAD model (right)

IV. Payload Design

A. Laser Ablation to Clear Micro Debris

To redirect the debris particles, small amounts of mass are to be ablated from the particles using the laser system. For this mission, the objects are assumed to be aluminum and have similar absorption characteristics. With sufficient power, the laser will be used to rapidly ablate mass in pulses. The ablated mass will be ejected from the particle with significant velocity, which causes an appreciable change in momentum on the particle. While in-depth studies and models on ablative characteristics of aluminum as a function of laser wavelength, pulse frequency, and power are limited, one paper from Choi and Pappa found an ablation rate of 3 mg per 100 J input of power while using a UV laser with 1 microsecond pulse width [3]. This was also found to have a plasma plume ejection of between 10 and 100 km/s [3]. These values helped to drive the selection for a laser, while also providing a preliminary forcing model for a physical simulation of debris trajectory changes.

B. Laser and Target Monitor

1. Laser Design

Optimizing a laser design is crucial to ensure a feasible mission. An optimal laser minimizes the time to deorbit the microdebris while fitting within the constraints of the mission—in particular, the size, mass, power, and thermal constraints. The time to deorbit a microdebris particle is a convoluted function that depends on many variables including the material properties, mass, and orbital dynamics of the particle, as well as the laser properties and consequent ablation physics. Determining the trends between time-to-deorbit and variations in these properties for optimization requires extensive simulations due to the nonlinear and complex nature of the physics, an area of future work. However, to progress the research of this field, the team has analyzed the datasheets of over 300 commercially-available laser systems to determine how laser parameters such as average power, wavelength, pulse energy and peak vary with the size (largest dimension), mass, and cooling system of the laser. Fig. 5 and Fig. describe these trends, as well as the mass and size constraints for this mission, to contribute to determining the most optimal laser. These figures establish the bounds of current laser feasibility in the industry, once future work can correlate the laser parameters

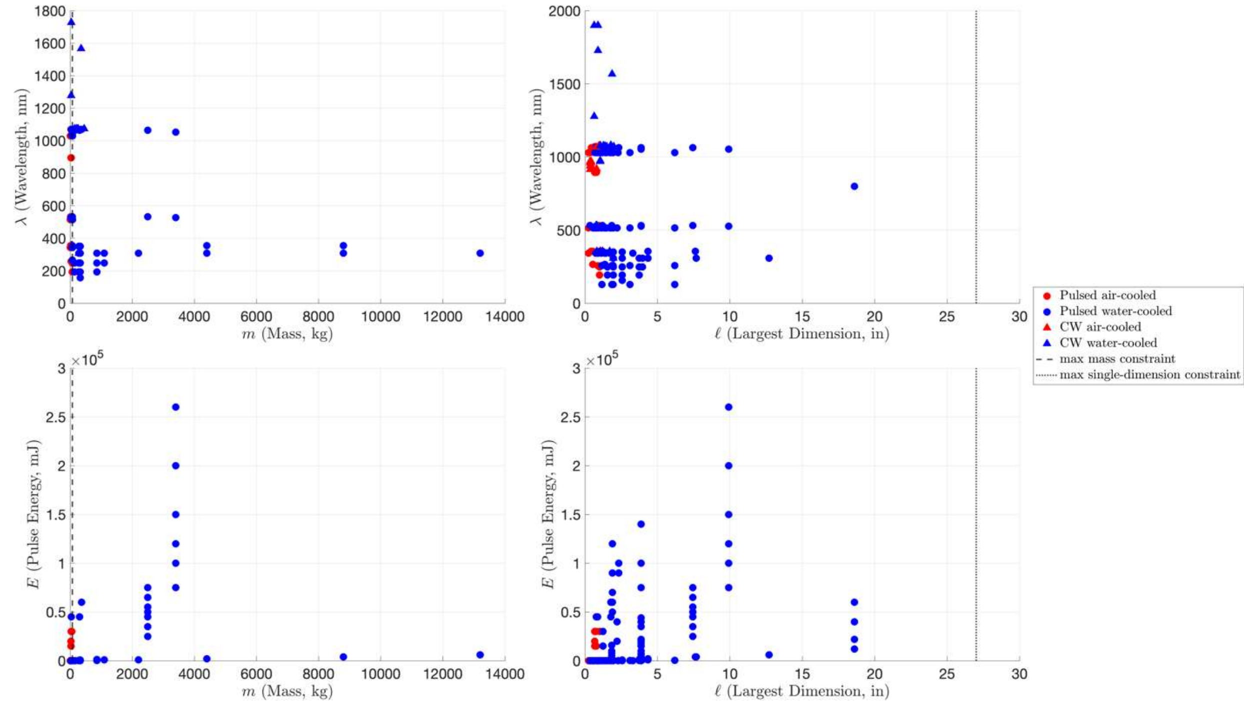

Fig. 5. Wavelength and pulse energy vs. laser mass and largest dimension for existing industrial lasers [4-8].

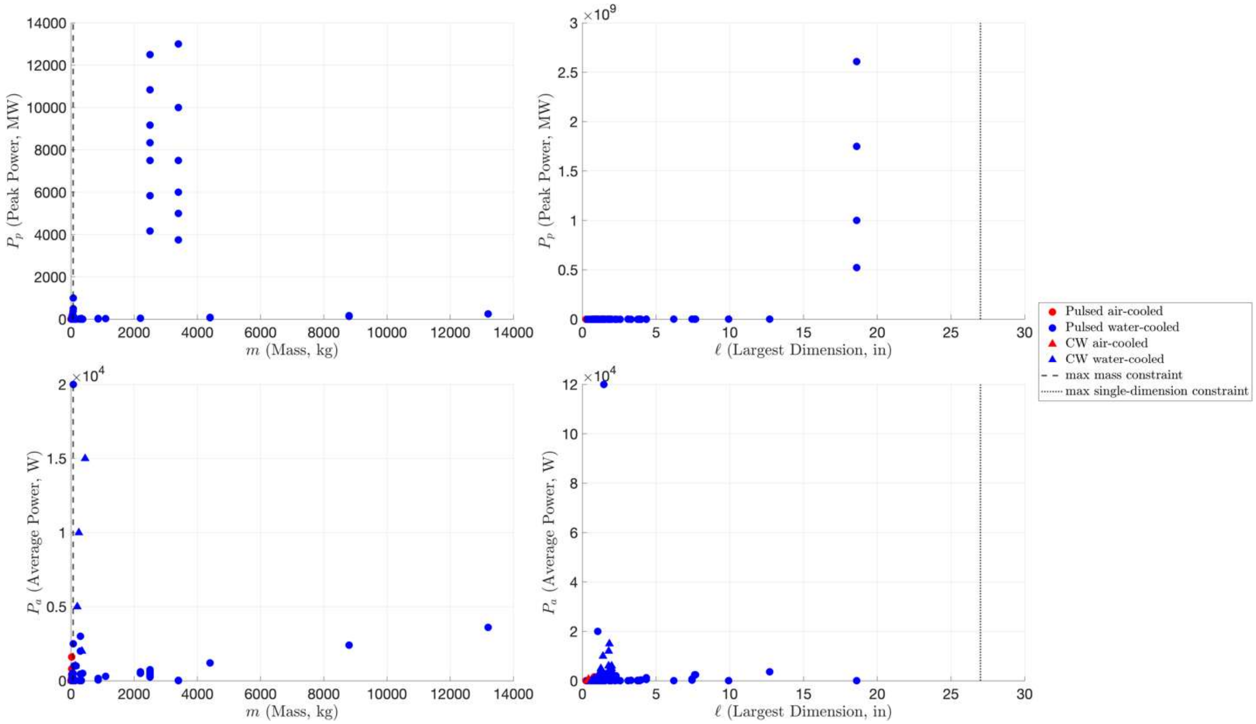

Fig. 6 Peak and average power vs. laser mass and largest dimension for existing industrial lasers [4-8].

2. *Target Monitor Design*

The target monitor was resolved with a trade study based on the tracking-distance and fidelity requirements for microdebris prescribed by Fig., to maximize the number of microdebris encounters per year. Table 5 and Table then provide a trade study based on estimated criteria ranges. Since a radar is expected to be used on the ground station to find clouds of microdebris, as well as the dish size for a radar, lidar types were preferred over radars. The most optimal lidar is found to be the twin fan sweep lidar, which can determine microdebris position and velocity as microdebris passes through the lidar and reflects light. To help observe the reflected light, an infrared camera has been selected.

The selected target monitoring system is analogous in concept to the configuration of the long-range precision lidar of the NASA ICESat-2, which instead uses a telescope to detect the reflected light (besides a different kind of lidar for different mission purpose) [16].

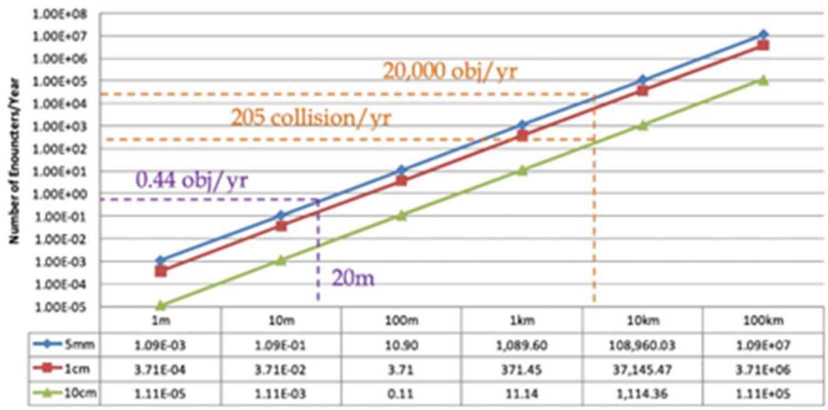

Fig. 7 Encounters per year by effective diameter at 850 km altitude [1].

Table 5 Target monitor: trade study legend.

Label	Score	1	2	3	Units	Description
T1	*Range*	< 10	10 – 50	> 50	km	-
T2	*Precision*	> 10	1 – 10	< 1	% Error	Error in the data output from true values
T3	*Required Power*	> 500	500 – 250	< 250	W	Power required by device
T4	*Detection Size*	> 10	10 – 1	< 1	cm	Size of microdebris
T5	*Average Size*	> 4000	4000 – 100	< 100	in^3	Size of device
T6	*Average Mass*	> 50	50 – 10	< 10	kg	Mass of device
T7	*Lifespan*	< 3	3 – 5	> 5	Years	-
T8	*TRL*	< 4	4 – 6	> 6	TRL	-
T9	*Cost*	> 5	5 – 1	< 1	$Million	-
T10	*Robustness*	No Protection	Moderately Hardened	Hardened	Radiation Hardness	How resilient is it to space weather?
T11	*Data Rate*	> 10	1 – 10	< 1	Gbps	Onboard processing / bandwidth needed
T12	*Duty Cycle*	< 30	30 – 70	> 70	Percent	Continuous operation capability
T13	*Cooling*	Active	Passive	None	Cooling	-
T14	*Field of View*	< 10	10 – 60	> 60	°	-
T15	*Autonomy (Information processing)*	Computer Vision	Filtering Processing	Basic Math	-	How much help do you need / can it process all the data on its own easily? Does it need AI?
T16	*Low-light performance*	Low	Medium	High	Performance	Low = Requires direct illumination, Medium = Limited low-light capability, High = Fully functional in total darkness
T17	*Frame rate*	< 1	1 – 10	> 10	FPS	What is the rate at which it checks for change?
T18	*Amount of information extracted*	1	2	≥ 3	Sets	1 = position; 2 = position + velocity; 3 = position + velocity + thermal; etc.

Table 6 Target monitor: trade study matrix.

	Criteria (Label)	**T1**	**T2**	**T3**	**T4**	**T5**	**T6**	**T7**	**T8**	**T9**	**T10**	**T11**	**T12**	**T13**	**T14**	**T15**	**T16**	**T17**	**T18**	**Total**
	Weights	*15%*	*10%*	*2%*	*15%*	*5%*	*2%*	*1%*	*5%*	*1%*	*5%*	*5%*	*5%*	*5%*	*10%*	*5%*	*5%*	*2%*	*2%*	*100%*
Lidar	*Doppler*	3	2	2	2	2	3	3	3	2	3	2	3	2	2	3	3	2	2	81%
	Frequency Modulated Continuous Wave (FMCW)	3	3	1	3	2	2	3	3	2	2	2	2	1	2	3	3	2	3	84%
	Flash	2	2	1	2	2	2	3	3	2	2	2	2	1	2	3	3	3	2	70%
	Twin Fan Sweep	3	3	1	3	2	2	3	3	2	2	2	2	1	3	3	3	2	2	86%
	Multispectral	3	3	1	3	2	2	3	2	2	2	2	2	1	2	3	3	2	3	82%
	Hyperspectral	3	3	1	3	1	2	3	2	1	1	1	1	1	2	3	3	1	3	74%
	Polarmetric	2	2	2	2	2	2	3	3	2	2	2	2	2	2	3	3	2	2	72%
Radar	*Phased Array*	3	3	2	2	2	1	3	3	2	3	2	3	2	3	3	3	2	2	86%

	Doppler	3	2	2	2	2	2	3	3	2	3	2	3	2	3	3	3	2	2	84%
	Sythentic Aperture (SAR)	3	2	2	2	2	2	3	3	2	3	2	3	2	2	3	3	1	3	80%
	Inverse Synthetic Aperture (ISAR)	3	2	2	2	2	2	3	3	2	3	2	3	2	2	3	3	1	3	80%
	Passive	2	1	3	1	1	1	3	2	3	2	3	2	3	3	3	2	2	1	65%
	BiStatic/Multistatic	3	2	2	2	2	2	3	3	2	3	2	3	2	3	3	3	2	2	84%
Infrared Camera	*Shortwave Infrared (SWIR)*	2	2	2	2	2	2	3	3	2	2	2	2	2	2	2	2	2	2	69%
	Midwave Infrared (MWIR)	2	2	1	2	2	2	3	3	2	2	2	2	1	2	2	2	2	2	66%
	Longwave Infrared (LWIR)	2	2	1	2	2	2	3	3	2	2	2	2	1	2	2	2	2	2	66%
Other Camera	*Passive / Visible Optical*	2	2	2	2	2	2	3	3	2	2	2	2	3	2	1	1	2	1	66%
	Polarimetric	2	2	2	2	2	2	3	3	2	2	2	2	2	2	1	1	2	2	65%
	Stereoscopic	2	2	2	2	2	2	3	3	2	2	2	2	3	2	2	1	2	2	69%

C. Thermal and Power Systems

The Thermal and Power subsystems are both very crucial to the operation and survivability of the spacecraft and payload. The first subsystem to be examined was power since all subsystems and components are affected, and certain components in the power subsystem will generate/require different thermal conditions. It was determined through the power budget analysis and laser analysis how the power setup would be configured. The laser itself will draw power from a setup of 12 supercapacitors. The setup will have 4 rows and 3 columns. The three supercapacitors in each row are in series while the 4 in each column are in parallel. The battery module has a similar set up with 8 lithium-ion batteries. The configuration is four rows of two batteries. The two batteries in each row are in series with the four in the columns in parallel. Using general equations of the physics of electricity allowed for calculating the effective specs of the battery and supercapacitor configurations [9,10].

Table 7 Battery module and supercapacitor parameters.

Battery Module	
Parameter	**Value**
Capacity	288 Ah
Energy	2073.6 Wh
Weight	16.792 kg
Charge Current Limit	144 A
Discharge Current Limit	288 A
Operating Temp. Range	10°C to 30°C
Storage Temp. Range	-5°C to 5°C

Supercapacitors	
Parameter	**Value**
Capacitance	133.33 F
Voltage	9 V
Energy	1.5 Wh, 5400 J
Operating Temp. Range	-40°C to 65°C

The battery module is used to charge the supercapacitors. This is done using a DC-DC boost converter limited to 100 Watts because the supercapacitors hold more voltage than the batteries. It achieves this charge in twenty minutes or less. Twenty minutes is a bit high for the charge time, but it was done to avoid over production of heat. The supercapacitors, after reaching full charge, will also use a boost converter to discharge their energy for the laser's use. The laser is used to ablate and move the debris. Accounting for a loss, the effective available voltage from will be 8.1 Volts. The voltage that can effectively be passed by the supercapacitors is 4.5 Volts. Using

$$E = \frac{1}{2}C\left(V_{max}^2 - V_{min}^2\right) \text{ and } t = \frac{E}{P}, \tag{1,2}$$

the energy was found to be .84 Wh and the max activation time for the laser is 61.2 seconds.

Next, was finding lidar power consumption. The lidar is rated for 1000 Watts of power and is activated for one hour to ensure sufficient target tracking and confirm an ablation event occurred. Accounting for inefficiencies, the energy used ends up being 1111.1 Watt-hours. The boom motors and galvo box consume a negligible amount of the battery module's energy. The infrared camera is rated for 25 Watts and will be active for as long as the lidar. This results in the lidar using 25 Watt-hours of the battery module's energy.

This is when some thermal analysis occurred. After conducting thermal analysis, which will be discussed in more detail after power, there will be active cooling of 75.4 Watts for 70 minutes and active heating of 59.81 Watts for 33 minutes. This will result in 88 Watt-hours of active heating and 59.81 Watt-hours of cooling. The active cooling will be used during payload activation meaning that after one full cycle of being in the sun and laser firing, there will be 849.28 Watt-hours left in the battery module which is about 40% of battery charge. One can see this in Figure 8.

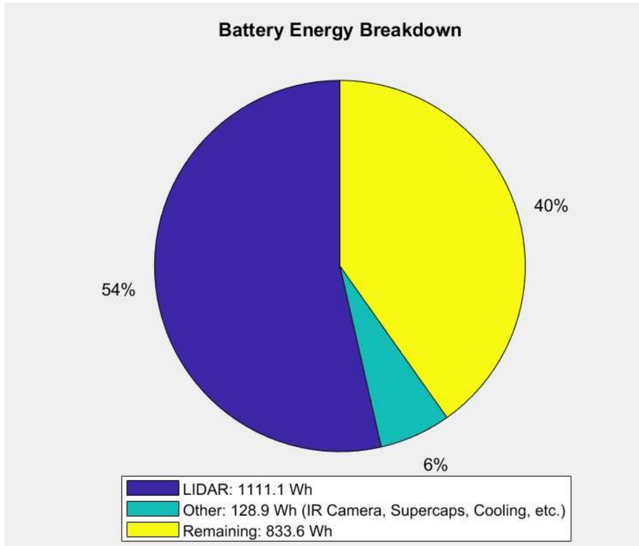

Figure 8 Battery energy usage.

Now to address the thermal systems. The first step was to use the eclipse times to determine the amount of time the spacecraft spends in shadow and how much time it spends in the sun. This can be seen in Figure 8 This sun exposure along with the heat generated by power use in the payload generates a total heat load into the system of 353 Watts. One side of the payload is open to radiate directly into space with an area of .18 square meters. Two sides of the payload sleeve have Starsys louvers with an area of .6 square meters. This gives a combined radiative area of .78 square meters. The passive cooling from this radiative heat dissipation can bring the payload's equilibrium temperature to 38.1 Celsius. With the active cooling mentioned earlier in this section, that equilibrium temperature can be bought down to 20 Celsius. Thermal control during eclipse is also very important to ensure that the payload's components stay above catastrophically low temperatures. Before active heating is added, the equilibrium temperature is -73 Celsius which will require heating. The target temperature was set to be 15 Celsius for equilibrium and entered the Stefan-Boltzmann Law to find a required heating power of 59.81 Watts. This is the only power being used in the payload during eclipse leaving plenty of energy in the battery for heating the bus, comms, propulsion, etc. Figure 9 shows the active heating energy requirement intersecting with emission at the desired temp to indicate that the heating energy use is correct.

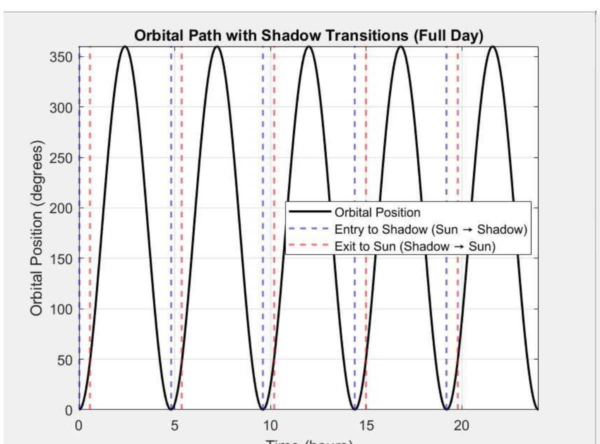

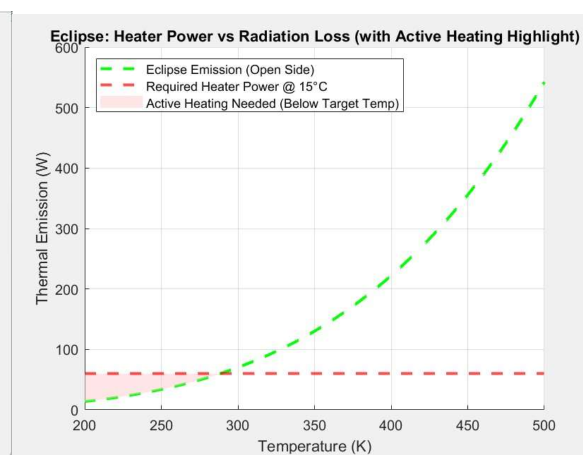

Figure 9 Eclipse times (right) and heater power (left).

V. Orbital Analysis and Physical Simulation

The orbital analysis subsection of the project consists of the analysis work for determining orbital parameters, building a Δv budget, and modelling the effects of laser ablation on the trajectory of debris particles. The tools used for these analyses are primarily numerical models implemented with MATLAB and Ansys Systems Tool Kit, with some analytical computations as well. Analyses covered in this section were used to drive design considerations in several other subsections of the project, but primarily in propulsion, communications, and ground station.

A. Orbital Parameters

The parking orbit parameters of the *Watchdog* mission are detailed in Table 8. These parameters were driven by considerations of other subsystems, such as the launch vehicle, and background research of micro debris altitudes.

Table 8 Parking orbit parameters.

Semimajor Axis	7228 km
Eccentricity	0
Argument of Perigee	0 deg
RAAN	260 deg
Inclination	28.5 deg
Orbital Period	102 minutes

It is expected that an easterly launch from Cape Canaveral will bring the spacecraft into an operating orbit of 28.5 degrees inclination. There is no need for an eccentric parking orbit in this mission, hence the orbit is circular (eccentricity is zero). As found through background research, the optimal altitude was 850 km, where debris of 10 cm size is most common [1]. This consideration constrains the semi-major axis of the orbit. The Right Ascension of the Ascending Node (RAAN) was determined based on the epoch time of mission launch on April 15, 2025, 15:00:00 UTC.

B. STK Trajectory and Δv Analysis

Ansys Systems Tool Kit (STK) was used for backchecking Δv computations and trajectory changes for small orbital adjustments expected throughout the mission. Additionally, STK assisted other subsystems for their analyses. For example, eclipse times were generated in STK, then used by the power subsystem. It is expected that during the mission, new concentrations of debris will be near the mission orbit using the Space Fence radar. When found, *Watchdog* will be ordered to rendezvous with these concentrations and wait for encounters. To help size the propulsion system, an example rendezvous procedure was used to find Δv requirements.

A secondary "Waypoint" object is in orbit near 922 km altitude and is used as a test to rendezvous with a possible debris concentration. It is located at the same inclination as *Watchdog*, but a slightly higher altitude and leading the orbit. The purpose of rendezvousing would be to increase the likelihood of a close debris encounter.

The standard procedure for rendezvousing with a target would be to lower the orbital altitude if *Watchdog* is trailing and raise the orbital altitude if it is leading. A Hohmann transfer is performed to either raise or lower the orbits, with the lower bound of altitude being 700 km, and the upper bound at 1000 km. The spacecraft would then wait for a transfer window and perform a second Hohmann transfer to intercept the waypoint.

It is calculated that each Hohmann transfer (transfer from either 850 km to 700 km or 1000 km) will be two impulses of about 40 m/s, totaling 80 m/s. In this case, the Δv breakdown is described in Table 9. A more detailed breakdown of Δv is described in the Propulsion section. In addition, it is expected that these transfers will occur multiple times throughout the mission.

Table 9 Δv breakdown.

Description	Δv (m/s)
Impulse 1 (Xfer)	39
Impulse 2 (circularize)	39
Hohmann Xfer (to 700km)	78
Impulse 3 (Xfer)	57
Impulse 4 (Circularize)	58
Hohmann Xfer (to Waypoint)	115
TOTAL TRANSFER:	193

To illustrate the path of the satellite in orbit, Fig. 10 shows the launch from Cape Canaveral into the parking orbit, shown in green. The orbit is reduced in altitude to the purple 700 km orbit. Then, after waiting for a transfer window, the orbit is increased to the 922 km yellow orbit. The Waypoint marker shows the target orbital position, which starts leading the spacecraft.

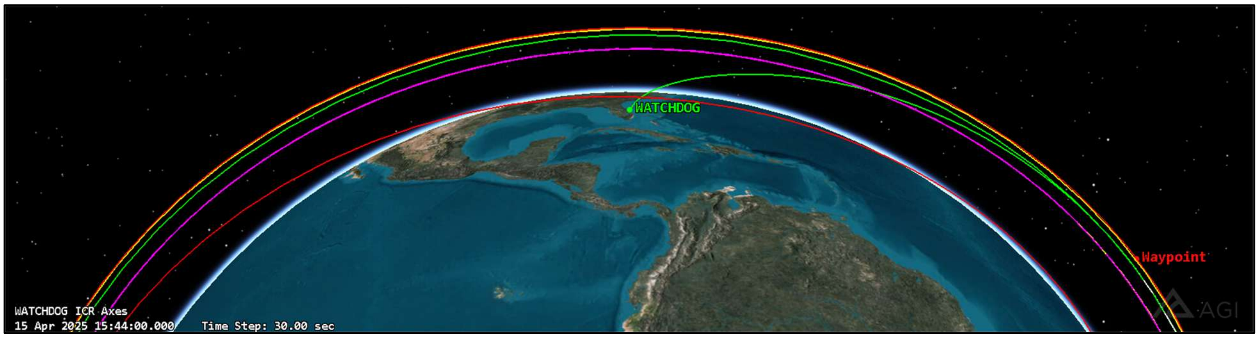

Fig. 10 STK graphic of astrogator orbital paths.

Further analysis is performed in STK to determine access times of the two ground stations. These analyses help determine access durations and frequencies throughout the mission.

C. Debris Trajectory Simulation

To investigate the feasibility and effect of ablating debris to alter its trajectory, a numerical model was developed in MATLAB. The model combines analytical and numerical orbit propagation techniques to output position and velocity information of debris particles.

To simplify the model, it is assumed that the laser has perfect targeting, and that there is sufficient power at the point of a close encounter to apply the ablation force over a time interval specified in the code. The ablation rate is also assumed to be constant, and the laser power is an average over the span of the simulation time step.

The phases of the simulation are detailed in Fig. 11. The orbit of the *Watchdog* satellite and a piece of debris are propagated based on an initial condition input. Over some span of time with a given time step, the orbits are propagated using point-mass analytical orbit methods while a relative position vector $\overrightarrow{\Delta r}$ has a magnitude greater than some threshold distance $R_{threshold}$. If within the threshold, the two objects are in a close encounter, and the simulation swaps to a numerical propagation using the equations of motion for a two-body simulation, with the addition of an ablation force on the debris particle. This force is a simulated ablation force which may be constant or variable and is only applied if the force is applied opposite the velocity vector of the debris. After a preset amount of time, the close encounter ends, and the ablation force is no longer applied. The ending conditions of this close encounter are used as the new initial conditions for the point mass propagation and the cycle continues until another close approach occurs.

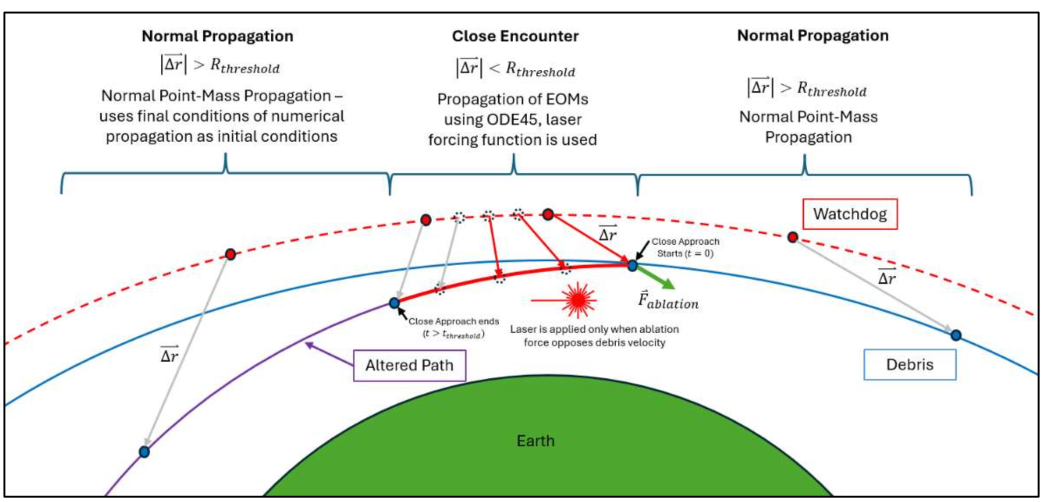

Fig. 11 Graphic of orbital laser redirection model.

For the duration of the close approach, the positions of the satellite and the close debris are propagated using the following equation of motion:

$$\vec{F_i} = -(GM_E m_i/r_i)(\vec{r_i}/r_i) = m_i\ddot{\vec{r_i}}, \tag{3}$$

an additional force, due to the ablated material, is added to the debris total force:

$$\vec{F}_{ablation} = (\dot{m}V)_{ablation}(\overrightarrow{\Delta r}/\Delta r), \tag{4}$$

where $(\dot{m}V)_{ablation}$ is the time rate of momentum change (force) caused by the ablation, which is assumed to be a constant mass change multiplied by the velocity of the ejected plasma. The mass ablation is a function of the average power of the laser over the time step of the simulation (1 second), the ablation rate is 3 mg per 100 J and the velocity of the ejected material is assumed to be constant 10^4 m/s [3]. By multiplying ablation rate by the power of the laser, the rate of mass ejection can be determined. The direction of this force is assumed to be along the direction from the satellite to the targeted debris ($\overrightarrow{\Delta r}$). For the simulation, the force is only applied if it is opposing the direction of motion of the debris, meaning it will decelerate the object. These equations of motion are propagated using the ode45 function.

Outside of the close approach, a point-mass propagated orbit is used. A set of initial conditions drives the beginning propagation. After a close approach, the final conditions of the debris are used to propagate a new orbit. These two-body solutions are computed using the Lagrange F and G solution. The reason for swapping to an analytical solution, rather than using numerical methods is for calculation simplicity. The code is intended to run for long time spans because close approaches may not be often, depending on the initial conditions of the simulated objects. Fig. 12 shows the results of a short test case, where a debris particle in a slightly lower orbit to the satellite catches up for an encounter.

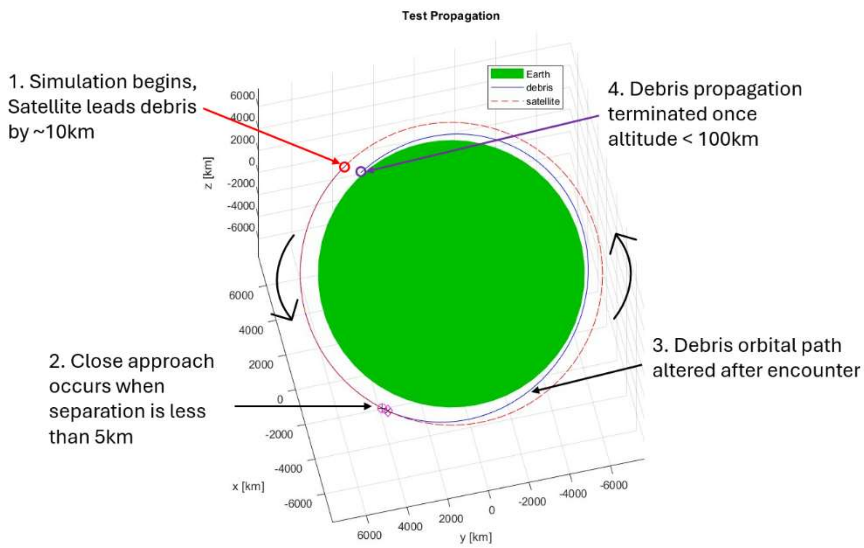

Fig. 12 Output of MATLAB simulation.

This simulation also uses a laser power output of 1.3 kW, which applies a force of approximately 0.4N to a 100g particle over a 40 second encounter. After the encounter, the debris is redirected onto another orbital path with a perigee less than 100 km. Effectively, the encounter has caused the debris to slow to a point where it may enter the atmosphere. If the altitude falls below 100 km, the particle will no longer be propagated, as it is assumed the orbit completely decays at that point.

VI. Spacecraft Bus Integration and Analysis

A. Blue Canyon Technologies Venus X-Class Bus

The selected Venus X-Class Bus configuration is the dual-configuration which produces 444 W of power with an available payload volume of 20’’x17’’x16.4’’[12]. The mass of the bus alone is 100 kg, while the maximum payload weight capacity of 70kg. The bus will utilize an ESPA ring around its lower edge to interface with the payload, a rectangular prism with the inner dimensions listed above.

An assumption, or modification for the bus is that the difference between its outer and inner walls diameter lies between 0.25 inches and 0.3 inches for the sake of attaching fasteners between the walls and each bolted component. UTS hole size #10-32 shall be used to fasten the payload to the outer boundary of the available volume. Loose wiring shall be secured via epoxy to the inner walls of the bus.

B. Launch Vehicle and Propulsion

In this section, an overview of the launch vehicle with structural considerations and the propulsion system onboard the bus are discussed.

3. Launch Vehicle and Structures

The Minotaur IV from Northrop Grumman is the designated launch vehicle for the *Watchdog* mission. The trade study that resulted in this decision focused on the importance of a cost-effective and reliable vehicle that met the mass and volume requirements for hosting the Venus X-Class Bus. The study ranked the reliability for each vehicle considered (Falcon 9, Atlas V, Ariane 5 and Minotaur IV) out of five, equivalent to the launch success rate of each. The following percentage weights were assigned to the cost, reliability, mass and volume capabilities respectively: 45, 45, 5, 5. The low weight assignments for mass and volume were justified by the minimal need for a massive launch vehicle given the size and weight of the Venus Bus. The Minotaur IV has a 92-inch diameter fairing that connects to the Venus Bus via the NGIS 38-inch separation fitting, the 38-inch baseline payload cone and a custom payload adapter that mirrors the Minotaur V payload attachment fitting (PAF). These allow for the Minotaur IV to be attached to the bus while offering low shock and lightweight benefits [13]. The Venus Bus itself will sit on a spring-loaded plate with its center of mass (COM) within 12.5 cm of the Minotaur's COM.

A structural analysis model for load, vibrations with finite-element method (FEM) can be built based on a system of equations and information provided from the Minotaur's User Guide. The guide provides standard figures for the Minotaur IV's sinusoidal, acoustic and shock environment as functions of payload mass. The shock and vibroacoustic environments take precedence over the sine vibration environment for total impact on the spacecraft. Analysis may be done using the average thrust forces of 500,000 lbf for the first stage, 275,000 lbf for the second stage and 65,000 lbf of thrust for the third stage. Further analysis can be made using the fundamental frequency and Von mises stresses for aluminum-focused analysis. The driving loads for stress analysis are launch vehicle loads. For the bus,

$$f_n = \frac{1}{2\pi\sqrt{\left\{\frac{3EI}{ML^3}\right\}}} \tag{5}$$

Components such as actuators that exert a force caused by motion may use the force margin equation,

$$F_{margin} = \left[\frac{F_{avail}}{FS_{known}(\Sigma F_{known}) + FS_{known}(\Sigma F_{unknown})}\right]^{-1} \tag{6}$$

The factors of safety FS_{known} and $FS_{unknown}$typically fall between 1.25-1.5 and 3.0-4.0 respectively. $F_{unknown}$ accounts for variables that fluctuate depending on the environment, or with time [11].

Analysis on the bus to find the natural frequency would be better left as a future works finding, as measurements for the bus are completely unknown and would require additional information for obtaining accurate figures for the standard Venus Bus and its solar panels (with minimal physical changes) that WATCHDOG uses. SolidWorks or CATIA may be used in the future to create a rigid body mesh of the STEP CAD File. Primary analysis focus would be dedicated to the Venus Bus's interface to the Minotaur, the solar panels, payload components such as the laser and the Venus Bus as a whole. The model should be constrained at the center of the separation plane between the bus and the Minotaur. Node spacing may be about 1 inch within the mesh.

The fundamental frequency analysis was completed with the payload boom since its dimensions are entirely self-invented and does not have the proven reliability that the only other moving part, the rotating Lidar, does. The boom, comprised of aluminum 1060, has the following respective imperial values for inertia, mass, length, E and consequently the fundamental frequency: 702.2,7.7, 49, 10e6, 5.97Hz. Neglecting the unknown forces, the force margin would be about 1.3 assuming an available force of 120.4 lbf before failure, a known force of about 80 lbf and a FS of 1.5.

4. Spacecraft Propulsion System

A fast-acting propulsion system is necessary for this mission, as it is expected the spacecraft will need to rendezvous with debris areas and perform attitude adjustments often. The Δv requirements from Table 9 were used to drive a Δv budget. The details of this budget are show in Table 8.

Table 10. Δv budget.

Event	Δv (m/s)

Estimated Rendezvous Δv (2x Hohmann Transfers)	200
4 Total Rendezvous:	800
Orbit Sustaining (5 years)	0.5
End of Life Deorbit	240
Attitude Adjustment (10% prop. Mass)	82
TOTAL:	1122

It is assumed that the spacecraft will perform rendezvous with other orbital positions 4 total times. A very small amount is allocated for sustaining the orbit, and a margin is included to deorbit. As suggested by SMAD 1999, 10% more propellant mass is included for attitude adjustment, which provides 82 m/s more Δv [11].

The propulsion is a monopropellant hydrazine system 130N Force, with 230s Isp. The full hardware for this is expected to be 9.8 kg, with 93.9 kg of propellant included. It is assumed that several thrusters are included to allow for attitude correction in all directions.

C. Ground Station and Communications

A link budget was created for both uplinks and downlinks, as seen in Table . It was found that the downlink margin must be 4.4 dB, and the uplink margin must be 40.5 dB.

Table 11. Link budget downlink (left) and uplink (right).

	Downlink			Uplink		
Transmitter	Frequency	2.50	GHz	Frequency	2.65	GHz
	Antenna Power (W)	7000	mW	Antenna Power (W)	500	W
	Diameter	0.0838	m	Diameter	11	m
	Pointing Error	140	deg	Pointing Error	0.07	deg
	Antenna Power (dB)	8.45	dBW	Antenna Power (dB)	27.0	dBW
	Line Loss	-1.0	dB	Line Loss	-1.0	dB
	Peak Gain	4.3	dB	Peak Gain	47.1	dB
	Pointing Loss	-23.4	dB	Pointing Loss	-0.1	dB
	Transmit Gain	-19.1	dB	Transmit Gain	47.0	dB
	Net Gain	-11.7	dB	Net Gain	73.0	dB
Receiver	Diameter	11	m	Diameter	0.0838	m
	Pointing Error	0.07	deg	Pointing Error	140	deg
	Peak Gain	46.6	dB	Peak Gain	4.74	dB
	Pointing Loss	-0.1	dB	Pointing Loss	-26.3	dB
	Net Gain	46.5	dB	Net Gain	-21.6	dB
Other	Path Length (max)	1000	km	Path Length (max)	1000	km
	Space Loss	-160.4	dB	Space Loss	-160.9	dB
	Bit Error Rate	1.0E-05		Bit Error Rate	1.0E-05	
	Modulation	BPSK, R-1/2 Viterbi		Modulation	BPSK, R-1/2 Viterbi	
	E_b/N_0 Reqd.	10.9	dB	E_b/N_0 Reqd.	4.5	dB
	Imp. Loss	-2.0	dB	Imp. Loss	-2.0	dB
	Prop./Polarization Loss	-0.03	dB	Prop./Polarization Loss	-0.03	dB
	Data Rate	12.1	Mbps	Data Rate	120	kbps
	Noise Temp.	135	K	Noise Temp.	135	K
	Link Margin:	4.4	dB	**Link Margin:**	40.5	dB

The ground stations chosen are critical to mission success. There will be three ground stations used; the Space Fence radar located in the Republic of the Marshall Islands, the Malabar transmitter located in Brevard County, Florida, and Awarua Ground Station located in New Zealand. The Space Fence Radar employs S-band radar technology to detect and monitor debris as small as 10 centimeters in low Earth orbit [14]. It will be used for continuous monitoring and real time data collection, but there is no technology for communication. The Malabar transmitter is located near the launch site, Cape Canaveral, which allows for coordination with launch operations. It also has essential communication infrastructure, telemetry, and tracking that will ensure mission success. The third, and final, ground station is the Awarua Ground Station. This ground station has geographical advantages for covering polar and inclined orbits, and while specific capabilities are less documented, there are existing communication infrastructures, and technologies that support satellite tracking [15].

D. Command and Data Handling (C&DH) and Guidance, Navigation and Control (GNC)

Command and data handling combines telemetry from multiple sources and processes it for downlink or internal spacecraft use. Fig. 13 shows the spacecrafts data handling unit.

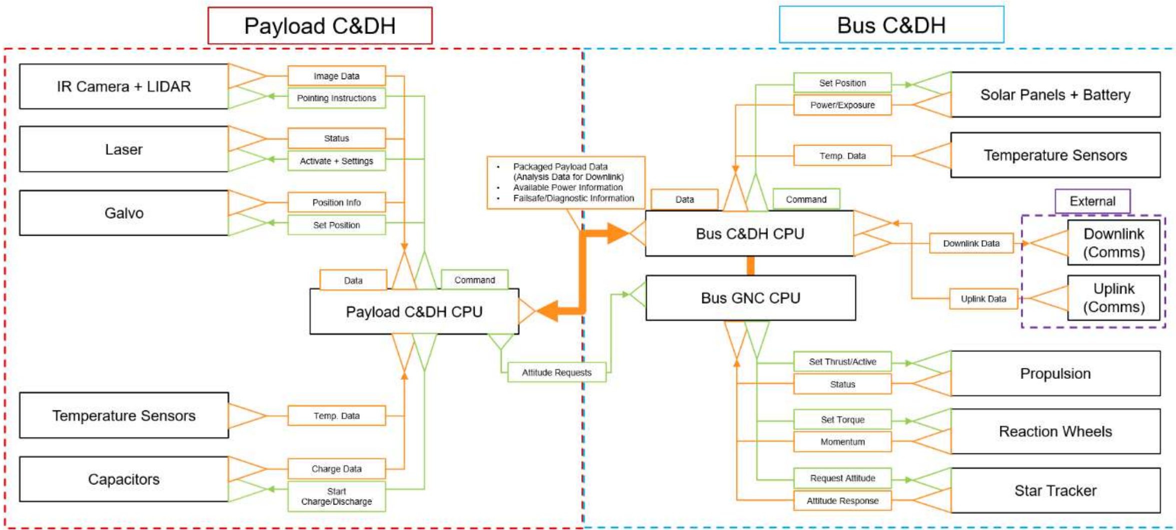

Fig. 13 Command and data handling unit block diagram

The Command and Data Handling (C&DH) Subsystem is essential for managing commands and processing data in the watchdog. It includes command sources like uplinks from ground stations and an onboard computer for execution, as well as hardline connections for testing. Key components feature sensors such as IR cameras and LIDAR for environmental monitoring and navigation, boom motors for appendage control, and thermal sensors to prevent overheating. Data processing is handled by dedicated CPUs for both payload and bus operations, processing high-level analog signals encoded as voltage in the range of 0 to 5.2V, as well as low-level analog signals with typical gain values of 100 to 300. Power is managed through solar panels and batteries, with photodiodes optimizing energy usage and actuators executing mechanical tasks. A feedback mechanism provides real-time data for monitoring and adaptive responses, ensuring robust task execution and reliable mission performance.

VII. Cost and Risks

To estimate the costs for the mission, the SSCM19 software, provided by Aerospace Corp., was used to generate a cost breakdown of the Venus bus subsystems. This model contains parametric models and cost estimating relationships to break down the subsystems cost. This cost estimate also couples with both the bus and the payload. By matching the input parameters with the design, considering mass, power, lifespan, propulsion, etc., the cost breakdown was generated and is displayed in Table 12. This breakdown includes only the unit cost of the systems.

Table 12 Spacecraft Bus Component SSCM19 cost estimation.

	Estimate (FY25$K)				**% of**	**% of**
	Non-Rec	*Rec*	*Total*	*Std Error*	*Sub-level*	*Sys-level*
Spacecraft Bus Subsystems						
Power	2,151	3,305	**5,456**	2,046	16.9%	
Structure	2,155	1,980	**4,135**	1,848	12.8%	
ADCS	2,000	2,201	**4,201**	1,500	13.0%	
Propulsion	712	1,377	**2,089**	932	6.5%	
TT&C*	2,300	2,255	**4,554**	5,039	14.1%	
C&DH*	4,867	4,772	**9,639**		29.8%	
Thermal	1,161	1,073	**2,235**	977	6.9%	
Spacecraft Bus	**15,346**	**16,963**	**32,309**	**6,088**	**100%**	62.5%
IA&T*	3,311	3,881	**7,192**	4,087		13.9%

PM/SE	4,288	5,166	**9,454**	5,077	18.3%
LOOS*	0	2,728	**2,728**		5.3%
S/C Development & First Unit	**22,945**	**28,738**	**51,683**	**8,919**	**100%**

The most likely risks encountered during the mission are outlined in Table 13. There are many risks with the mission, but for brevity, only the most prominent ones with the mission are displayed.

Table 13 Most Prominent Risks and Mitigation Methods

Risk	Pre-Mitigation	Post-Mitigation
1. Lasering a non-debris target	Without sufficient checking, the payload could laser objects that are not debris (C1)	Inclusion of an IR camera capable of distinguishing between debris and other objects (D4)
2. Pushing debris onto trajectories other than sub-orbital	If the laser were to ablate any particle found, it may push it in a direction that does not assist in deorbiting (B3)	The tracking system must verify the trajectory of the target before lasering to ensure it will move against its velocity (D3)
3. Regulatory risk with high-powered lasers in space	Some parties may not be comfortable with a debris-clearing satellite near operational satellites (C2)	Communicate with satellite hosts operating near Watchdog to ensure there are no conflicts (C4)

These risks are accompanied by Table 14, which shows the movement of severity and probability before and after mitigation, which corresponds to the numbering in Table 13.

Table 14 Risk Assessment Matrix

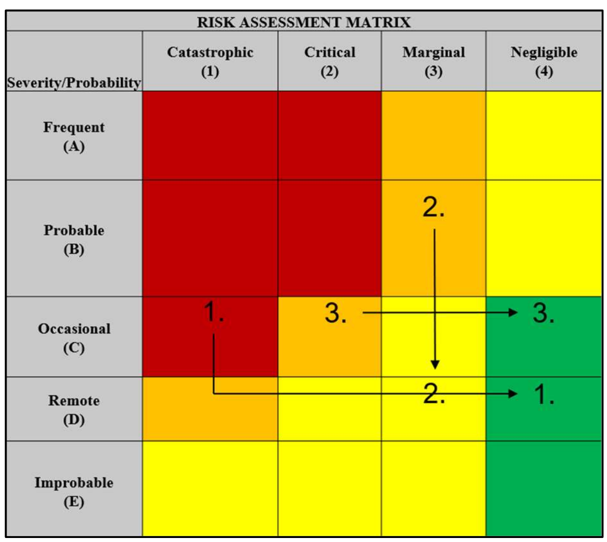

In addition to these risks, it is worth noting that many of the technologies used for the mission are not considered to be very high on TRL. Specifically, the laser, tracker, and thermal systems included on the payload are most likely to be near TRL 3-4. Moving forward with Preliminary Design Review (PDR), it would be best if either in-space or laboratory technical demonstrations for each separate technology were performed to help improve TRL and overall risk ahead of the full Watchdog mission.

VIII. Future Work

The future work for the project would include further simulations of the physical system, development of better ablative models, optimizing the required laser wavelength and frequency, and performing preliminary experiments or demonstrations to reduce risk for the lower TRL components. While a physical simulation was developed for experimenting with debris redirection, it would be best if many force and power inputs for the laser could be tested to find optimal design parameters for the laser. To help with this simulation, improved ablative models will help to relate laser power output to the rate of mass ablation, as well as the velocity of the material ejected from the particles. By incorporating accurate ablative models with the physical simulation, the best parameters for a laser may be found. Finally, to verify a laser selection, the chosen wavelength, frequency, etc. should be checked using real-world experiments, preferably on the ground and later in space to help raise TRL.

Each of these steps may be performed before or in parallel with a PDR. It would be best if this work be performed before PDR such that a better operational understanding of the mission can be achieved, while also reducing the risk for the proposed mission.

Acknowledgments

We thank Dr. Sara Lego and Dr. Sharad Sharan of Pennsylvania State University, as well as Edward Tate, CTO of Virtus Solis Technologies, for advising this project. We also thank Mr. Nicholas Cera for his contributions to the concept of operations and mission design.

References

[1] Pulliam, W., “Catcher's Mitt Final Report,” Defense Advanced Research Projects Agency.
[2] "Space Debris 101," Aerospace Corporation, 2024..
[3] Choi, S. H., Pappa, R. S., “Assessment Study of Small Size Space Debris Removal by Orbit-Stationed Laser Satellites”, Recent Patents on Space Technology 2, pp. 116-122, 2012.
[4] “Pulsed Lasers,” TRUMPF, URL: https://www.trumpf.com/en_US/products/lasers/pulsed-lasers/.
[5] “Nanosecond Lasers,” Amplitude, URL: https://amplitude-laser.com/products_category/nanosecond-lasers/.
[6] “Highpower Ultrafast Lasers,” Amphos, URL: https://www.amphos.de/.
[7] “Diode Lasers,” IPG Photonics, URL: https://www.ipgphotonics.com/products/lasers/diode-lasers.
[8] “Excimer Lasers,” Coherent, URL: https://www.coherent.com/lasers/excimer.
[9] “TVA Supercapacitors,” EATON.
[10] “72 Ah Space Cell,” Eaglepicher Technologies.
[11] Larson, W. J. et al., “Space Mission Analysis and Design,” 3rd edition, Microcosm Press, 1999.
[12] “2024 COSMIC Capstone Challenge Information Packet,” Consortium for Space Mobility and In-space Servicing, Assembly, and Manufacturing Capabilities (COSMIC), COSMIC-E01-WD001-2024-A, July 2024.
[13] Northrop Grumman, “Minotaur IV, V, VI User’s Guide,” Sept. 2020.
[14] Haimerl, J. A., and Fonder, G. P. "Space Fence System Overview." Lockheed Martin, Mission Systems and Training, Moorestown, NJ, 2015.
[15] “Awarua Satellite Ground Station,” Space Operations New Zealand.
[16] “ICESat-2 Ice, Cloud, and Land Elevation Satellite-2,” NASA, FS-2015-5-292-GSFC, URL: https://icesat-2.gsfc.nasa.gov/sites/default/files/page_files/FactSheet_0828_2018_0.pdf.